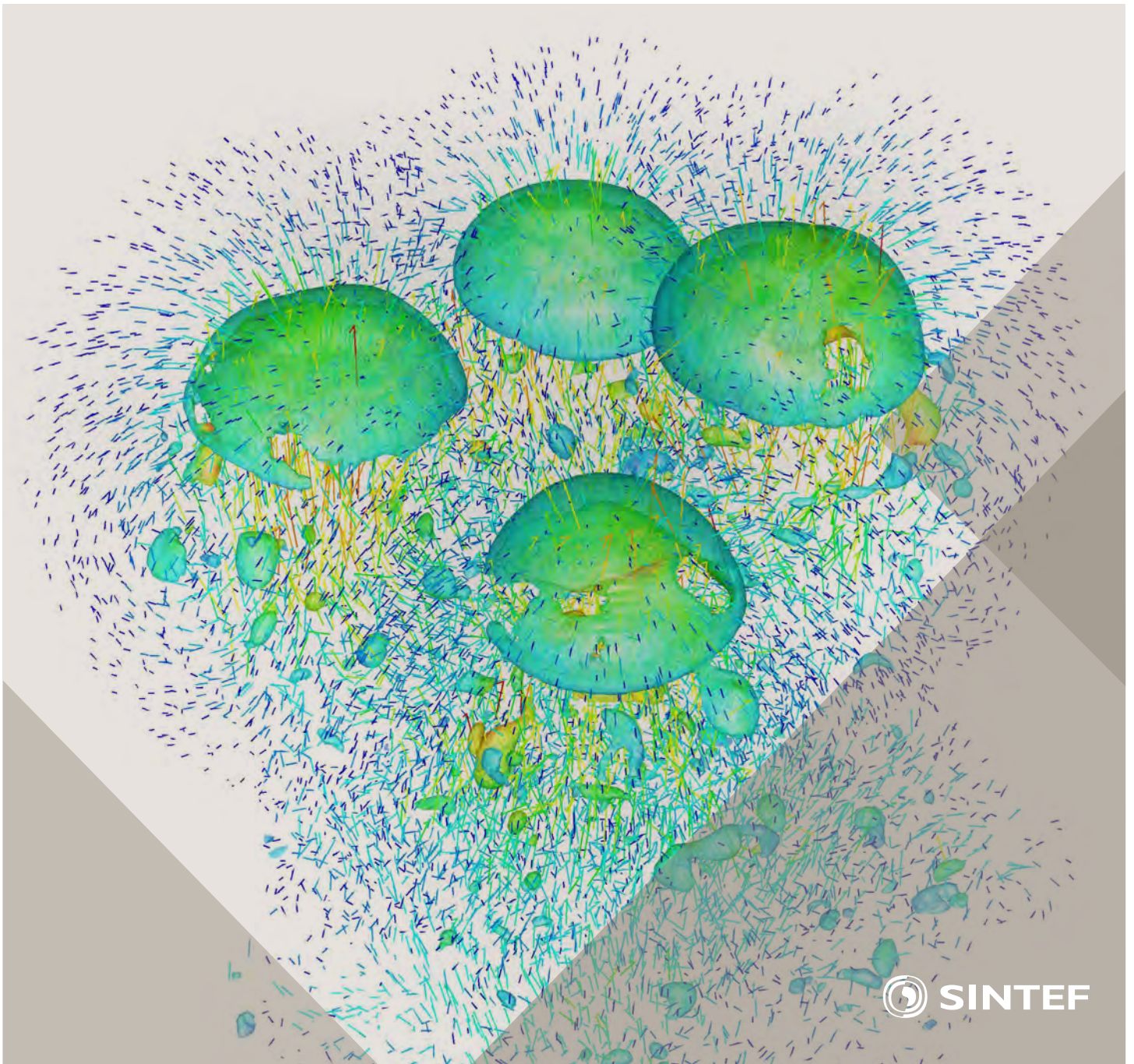


Selected papers from 10th International Conference on
Computational Fluid Dynamics in the Oil & Gas, Metal-
lurgical and Process Industries

Progress in Applied CFD



SINTEF Proceedings

Editors:

Jan Erik Olsen and Stein Tore Johansen

Progress in Applied CFD

Selected papers from 10th International Conference on Computational Fluid
Dynamics in the Oil & Gas, Metallurgical and Process Industries

SINTEF Academic Press

SINTEF Proceedings no 1

Editors: Jan Erik Olsen and Stein Tore Johansen

Progress in Applied CFD

Selected papers from 10th International Conference on Computational Fluid Dynamics in the Oil & Gas, Metallurgical and Process Industries

Key words:

CFD, Flow, Modelling

Cover, illustration: Rising bubbles by Schalk Cloete

ISSN 2387-4287 (printed)

ISSN 2387-4295 (online)

ISBN 978-82-536-1432-8 (printed)

ISBN 978-82-536-1433-5 (pdf)

60 copies printed by AIT AS e-dit

Content: 100 g munken polar

Cover: 240 g trucard

© Copyright SINTEF Academic Press 2015

The material in this publication is covered by the provisions of the Norwegian Copyright Act. Without any special agreement with SINTEF Academic Press, any copying and making available of the material is only allowed to the extent that this is permitted by law or allowed through an agreement with Kopinor, the Reproduction Rights Organisation for Norway. Any use contrary to legislation or an agreement may lead to a liability for damages and confiscation, and may be punished by fines or imprisonment

SINTEF Academic Press

Address: Forskningsveien 3 B
 PO Box 124 Blindern
 N-0314 OSLO

Tel: +47 22 96 55 55

Fax: +47 22 96 55 08

www.sintef.no/byggforsk

www.sintefbok.no

SINTEF Proceedings

SINTEF Proceedings is a serial publication for peer-reviewed conference proceedings on a variety of scientific topics.

The processes of peer-reviewing of papers published in SINTEF Proceedings are administered by the conference organizers and proceedings editors. Detailed procedures will vary according to custom and practice in each scientific community.

PREFACE

This book contains selected papers from the 10th International Conference on Computational Fluid Dynamics in the Oil & Gas, Metallurgical and Process Industries. The conference was hosted by SINTEF in Trondheim in June 2014 and is also known as CFD2014 for short. The conference series was initiated by CSIRO and Phil Schwarz in 1997. So far the conference has been alternating between CSIRO in Melbourne and SINTEF in Trondheim. The conferences focus on the application of CFD in the oil and gas industries, metal production, mineral processing, power generation, chemicals and other process industries. The papers in the conference proceedings and this book demonstrate the current progress in applied CFD.

The conference papers undergo a review process involving two experts. Only papers accepted by the reviewers are presented in the conference proceedings. More than 100 papers were presented at the conference. Of these papers, 27 were chosen for this book and reviewed once more before being approved. These are well received papers fitting the scope of the book which has a slightly more focused scope than the conference. As many other good papers were presented at the conference, the interested reader is also encouraged to study the proceedings of the conference.

The organizing committee would like to thank everyone who has helped with paper review, those who promoted the conference and all authors who have submitted scientific contributions. We are also grateful for the support from the conference sponsors: FACE (the multiphase flow assurance centre), Total, ANSYS, CD-Adapco, Ascomp, Statoil and Elkem.

Stein Tore Johansen & Jan Erik Olsen



Organizing committee:

Conference chairman: Prof. Stein Tore Johansen
Conference coordinator: Dr. Jan Erik Olsen
Dr. Kristian Etienne Einarsrud
Dr. Shahriar Amini
Dr. Ernst Meese
Dr. Paal Skjetne
Dr. Martin Larsson
Dr. Peter Witt, CSIRO

Scientific committee:

J.A.M. Kuipers, TU Eindhoven
Olivier Simonin, IMFT/INP Toulouse
Akio Tomiyama, Kobe University
Sanjoy Banerjee, City College of New York
Phil Schwarz, CSIRO
Harald Laux, Osram
Josip Zoric, SINTEF
Jos Derksen, University of Aberdeen
Dieter Bothe, TU Darmstadt
Dmitry Eskin, Schlumberger
Djamel Lakehal, ASCOMP
Pär Jonsson, KTH
Ruben Shulkes, Statoil
Chris Thompson, Cranfield University
Jinghai Li, Chinese Academy of Science
Stefan Pirker, Johannes Kepler Univ.
Bernhard Müller, NTNU
Stein Tore Johansen, SINTEF
Markus Braun, ANSYS

CONTENTS

Chapter 1: Pragmatic Industrial Modelling	7
On pragmatism in industrial modeling	9
Pragmatic CFD modelling approaches to complex multiphase processes.....	25
A six chemical species CFD model of alumina reduction in a Hall-Hérault cell	39
Multi-scale process models to enable the embedding of CFD derived functions: Curtain drag in flighted rotary dryers	47
Chapter 2: Bubbles and Droplets	57
An enhanced front tracking method featuring volume conservative remeshing and mass transfer	59
Drop breakup modelling in turbulent flows	73
A Baseline model for monodisperse bubbly flows	83
Chapter 3: Fluidized Beds	93
Comparing Euler-Euler and Euler-Lagrange based modelling approaches for gas-particle flows.....	95
State of the art in mapping schemes for dilute and dense Euler-Lagrange simulations	103
The parametric sensitivity of fluidized bed reactor simulations carried out in different flow regimes.....	113
Hydrodynamic investigation into a novel IC-CLC reactor concept for power production with integrated CO ₂ capture	123
Chapter 4: Packed Beds	131
A multi-scale model for oxygen carrier selection and reactor design applied to packed bed chemical looping combustion	133
CFD simulations of flow in random packed beds of spheres and cylinders: analysis of the velocity field	143
Numerical model for flow in rocks composed of materials of different permeability.....	149
Chapter 5: Metallurgical Applications	157
Modelling argon injection in continuous casting of steel by the DPM+VOF technique.....	159
Modelling thermal effects in the molten iron bath of the HIs melt reduction vessel.....	169
Modelling of the Ferrosilicon furnace: effect of boundary conditions and burst	179
Multi-scale modeling of hydrocarbon injection into the blast furnace raceway.....	189
Prediction of mass transfer between liquid steel and slag at continuous casting mold	197
Chapter 6: Oil & Gas Applications	205
CFD modeling of oil-water separation efficiency in three-phase separators.....	207
Governing physics of shallow and deep subsea gas release	217
Cool down simulations of subsea equipment.....	223
Lattice Boltzmann simulations applied to understanding the stability of multiphase interfaces.....	231
Chapter 7: Pipeflow	239
CFD modelling of gas entrainment at a propagating slug front.....	241
CFD simulations of the two-phase flow of different mixtures in a closed system flow wheel.....	251
Modelling of particle transport and bed-formation in pipelines	259
Simulation of two-phase viscous oil flow	267

MODELLING ARGON INJECTION IN CONTINUOUS CASTING OF STEEL BY THE DPM+VOF TECHNIQUE

Pavel Ernesto RAMIREZ LOPEZ¹, Pooria Nazem JALALI¹, Ulf SJÖSTRÖM¹ and Christer NILSSON²

¹ Swerea MEFOS AB, Box 812, SE-971 25, Luleå, SWEDEN

² SSAB EMEA, SE-971 88, Luleå, SWEDEN

* E-mail: pavel.ramirez.lopez@swerea.se

ABSTRACT

An advanced numerical model able to predict transiently the multiphase flow, heat transfer and solidification in a Continuous Casting mould based on the Volume of Fluid Method (VOF) in combination with the tracking of bubble trajectories during argon injection through a Discrete Phase Model (DPM) is presented. This methodology allows studying the effect of Argon injection on process stability; particularly, it investigates the influence of the bubble stream on steel/slag flow dynamics. Thus, different injection parameters such as bubble diameter and gas flow-rate were combined with specific casting practices to emulate industrial cases. As a result, the model makes possible the identification of stable or unstable flows within the mould under a variety of casting conditions (casting speed, nozzle submergence depth, etc.). Application to the industrial practice in a European Research Fund for Coal and Steel project is an ongoing task and preliminary results are illustrated. These results are fully applicable to explain the effect of gas injection on the behaviour of mould level fluctuations in the mould. Moreover, the predicted flow behaviour and bubble trajectories demonstrate good agreement with observed level changes, standing waves and gas departure positions observed on a physical model based on liquid metal and industrial observations. Ultimately, the increased process knowledge is used to optimize gas injection to provide a smooth distribution along the mould that benefits process stability. The robustness of the model combined with physical model observations make possible the description of phenomena difficult to observe in the caster, but critical for its performance and the quality of final products.

Keywords: Bubble dynamics, Argon injection, Discrete Phase Modelling, Volume of Fluid, Multiphase, Casting and solidification.

NOMENCLATURE

Greek Symbols

α Volume fraction
 μ Dynamic viscosity
 ρ Density
 σ Surface tension

Latin Symbols

C Non dimensional coefficient
 d Bubble diameter
 g Gravity
 Eo Eotvos Number
 F Force
 g Gravitational constant
 p Pressure
 T Temperature
 u Velocity
 V Volume

Sub/superscripts

b Bubble
 D Drag
 L Lift
 VM Virtual mass

INTRODUCTION

Argon injection is used during continuous casting to improve the removal of inclusions, which are transported by the argon-bubble stream to the slag bed; to be later assimilated in the liquid slag pool. A good deal of research has been done on this subject in the past 20 years, with mainly 2 numerical approaches to address the gas injection phenomena; namely Euler-Euler approach and Euler-Lagrangian approach (Cross *et al.*, 2006; Díaz *et al.*, 2008; Olmos *et al.*, 2001). The Euler-Euler approach requires tracking of two different sets of equations, one for the *continuum phase* (i.e. steel) and one for the *dispersed phase* (i.e. argon). The phases are solved as non-interpenetrating, immiscible media with their own material properties (density, viscosity, thermal conductivity, etc.) (Zhang *et al.*, 2006); thus, a complete set of flow equations (Navier-Stokes) is solved for each phase. In contrast, in the Euler-Lagrangian approach; the fluid is treated as a continuum by solving the Navier-Stokes equations, while the dispersed phase is solved in a “superimposed” way by tracking the bubbles through the calculated flow field. The dispersed phase can exchange momentum, mass, and energy with the fluid phase; but the trajectories of bubbles or particles are computed individually at specific intervals (i.e. particle or flow time step) during the continuum phase calculation.

Both methods have advantages and limitations. The Euler-Euler method is very accurate and normally favoured for analyzing flow columns with high volumes of gas (i.e. slug or annular flows, where the calculation of individual bubbles cannot be resolved or is not of particular importance, Figure 1).

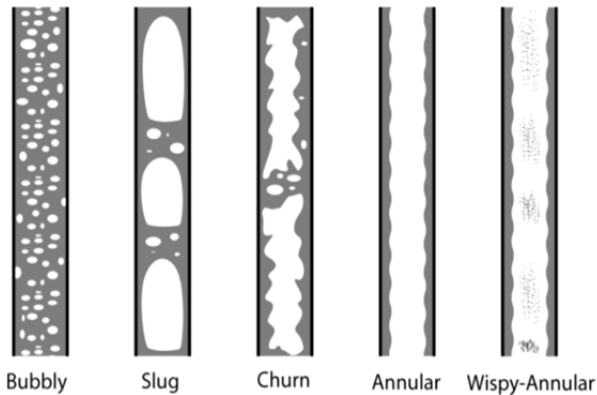


Figure 1: Different flow-gas regimes after Ghajar (Ghajar, 2005).

On the negative side, the Euler-Euler method is already computationally expensive for 2 phases and becomes unrealistically time consuming for a multiphase system such as the continuous casting process where slag, metal and argon are present. In contrast, the Euler-Lagrange method allows individual tracking of the bubbles at lower gas fractions, but former versions of the model used to be inaccurate when the dispersed phase occupied a large volume fraction ($\alpha_{gas} > 20\%$). However, improved versions of this approach are readily available in CFD codes such as ANSYS-FLUENT; which make it possible to account for higher gas fractions. These are called Discrete Phase Model (DPM) and Dense DPM model (ANSYS-Inc., 2013).

The DPM model allows more flexibility when coupled to other models such as turbulence, heat transfer and solidification. Moreover, DPM can be efficiently coupled to the Volume of Fluid (VOF) method to track the metal level (free surface) in a transient or steady mode. This VOF approach has been used successfully to track the evolution of the slag/metal interface on a model recently developed by the authors (Ramirez-Lopez *et al.*, 2010; Ramirez Lopez *et al.*, 2010). Nevertheless, the addition of a dispersed phase (argon) to the multiphase system (metal-slag) by DPM has not been tested before in CC modelling. Prior work has been done by Thomas *et al.* (Thomas *et al.*, 1997) and Pfeifer *et al.* (Pfeifer *et al.*, 2005) to use the DPM approach to simulate argon injection within the CC mould, but lacks the calculation of the free metal surface. Consequently, it was not possible to directly determine the effect of the gas on metal level stability or initial solidification at the meniscus. Recent application of the DPM technique combined with the VOF method to study metallurgical processes should be attributed to Cloete *et al.* (Cloete *et al.*, 2009; Olsen *et al.*, 2009) who applied the technique to analyze the stirring of steel ladles with argon. However, the slag phase is absent from the calculations. The use of the DPM+VOF

technique in this work is based on such work, but has been extended to account for the slag phase.

The fundamentals behind the DPM model can be found elsewhere and will not be reviewed in this manuscript. Instead, the present text is focused on the description of the modelling technique for adding argon injection to a multiphase-multiscale CC numerical model developed by the authors and validation of these predictions through experiments on a physical model with liquid metal and industrial observations.

BASE CONTINUOUS CASTING MODEL

The “base” CC model developed by the authors couples a multiphase steel-slag approach with heat transfer, mould oscillation and resultant solidification within the mould. The model uses the commercial code ANSYS-FLUENT v.14.5 to solve the Navier-Stokes equations together with the Volume of Fluid (VOF) method for calculation of the phase fractions (steel or slag) and the Continuum Surface Force (CSF) to account for surface tension effects in the meniscus (Brackbill *et al.*, 1992; Liow *et al.*, 2001). The κ - ϵ RNG turbulence model is used to capture flow turbulence, while heat transfer is solved through the Fourier equation. Heat extracted through the mould is calculated by a constant convection heat transfer coefficient based on the Nusselt number using typical water flow rates measured in the plants and a free stream temperature of 20°C. The heat flow through the slag bed is solved explicitly by addition of casting powder on top of the metal bulk and the calculation of the standard energy equation for a multiphase system in the VOF model. The boundary condition for powder feeding at the mould top depends on the industrial practice, being an air inlet if the slag bed does not fill the mould entirely; otherwise, a powder inlet is used. The slag-bed surface temperature measured with a thermal-camera is used as boundary condition at the mould top. Consequently, the thicknesses of the powdered, sinter and liquid slag layer are determined by the thermal conductivity of the slag as a function of temperature. Full details of the solution method have been published elsewhere (Ramirez-Lopez *et al.*, 2010; Ramirez Lopez *et al.*, 2010) and Figure 2 shows the boundary conditions used for the base model and argon injection.

Predictions include the calculation of the metal flow pattern inside the mould, the metal level height (i.e. metal-slag interface) as well as the behaviour of slag in the bed. The withdrawal of the solidified shell drags liquid slag into the gap to produce a slag film (i.e. lubrication or infiltration). The interfacial resistance between the solid slag and the mould or contact resistance due to the slag film as described by Spitzer *et al.* (Spitzer *et al.*, 1999) has been computed as a function of the powder’s basicity (Ramirez Lopez, 2010). This process is affected by casting conditions such as mould oscillation, powder composition, mould level control, rim formation, etc. Metal flow pattern predictions are shown in Figure 2b. These reveal typical flow structures such as jet and rolls but also the formation of a standing wave at the meniscus resulting from the particular SEN design.

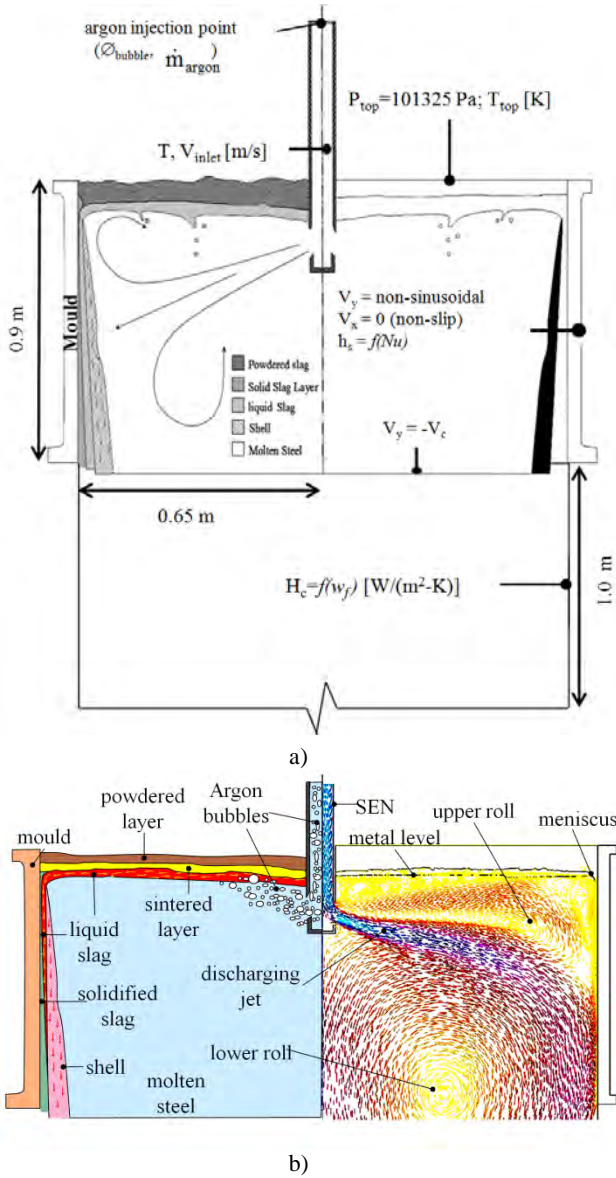


Figure 2: Numerical model for Continuous Casting, a) Boundary conditions used for base model and argon injection and b) Schematics of multiple phases present during casting (left) and typical metal flow predictions (right) after P.E. Ramirez Lopez et al. (Ramirez Lopez et al., 2013)

MODELLING ARGON INJECTION THROUGH THE DPM+VOF APPROACH

Although the fundamentals behind the DPM model can be found in the ANSYS-FLUENT v. 14 theory guide (ANSYS-Inc., 2013), some specific extra source terms (e.g. buoyancy, drag, lift, virtual mass and turbulent dispersion) were added as User Defined Functions (UDF's) (Cloete et al., 2009; Cloete et al., 2009; Olsen et al., 2009). Then, the momentum equation for the DPM model becomes:

$$\frac{du_b}{dt} = \frac{g(\rho_b - \rho)}{\rho_b} + F_D(u - u_b) + F_{VM} + F_L \quad (1)$$

where u is the velocity in x , y or z axis; ρ and ρ_b are the density of the bulk flow and bubbles and F_D , F_{VM} and F_L are the source terms for drag, virtual mass and lift, respectively.

The drag source term is defined as:

$$F_D = \frac{18\mu}{\rho_b d_b^2} \frac{C_D Re}{24} \quad (2)$$

where $C_D = 0.666\sqrt{Eo/3}$, which is a function of the Eotvos number. The virtual mass and lift source terms are defined as:

$$F_{VM} = \frac{1}{2} \frac{\rho}{\rho_b} \left(\frac{\partial u}{\partial t} - \frac{\partial u_b}{\partial t} \right) \quad (3)$$

$$F_L = C_D \rho_l V_b (u_l - u_g) \times (\nabla \times u_l) \quad (4)$$

Different approaches have been used and a variety of experiments have been performed to determine the evolution of drag and lift for bubble columns and single bubbles (Tomiyama, 2004); however, such discussion is beyond the scope of this work. The present approach is based on a combination of coefficients as suggested by Olsen et al. (Olsen et al., 2009). Regarding turbulence, prior work has highlighted deficiencies on early κ - ϵ formulations for tracking bubbly flows since turbulence is scaled on mean flow gradients rather than bubble size (Johansen et al., 1988). The *random walk model* was used to address this issue. This approach is a type of “eddy lifetime” model that describes the effects of small-scale turbulent eddies on bubbly flows by using a Gaussian distribution for the turbulent fluctuating velocities and a characteristic timescale for the eddies (ANSYS-Inc., 2013). The bubble size is determined from experiments by Iguchi et al. (Iguchi et al., 1995), where diameter of gas bubbles in liquid iron was proven to depend on the inner diameter of the injection pipe for stagnant flow conditions. The robustness and accuracy of the DPM+VOF technique was validated by comparing to an experimental benchmark (Deen et al., 2001; Zhang et al., 2006). The benchmark consists of a quadrangular base column of water, where air is supplied at the bottom with a given velocity, mass flowrate, bubble size, etc. Details of the benchmark are presented on Figure 3.

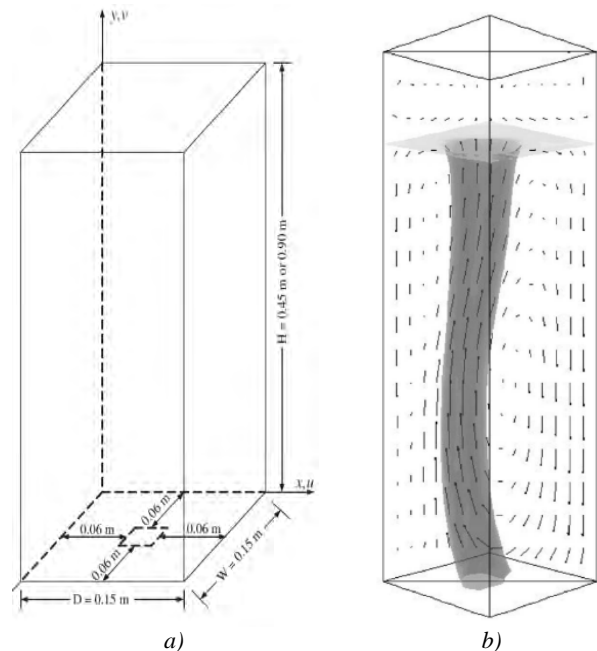


Figure 3: Bubble column experiment after (Deen et al., 2001; Zhang et al., 2006), a) Experiment dimensions, b) schematics of gas plume for experiments and simulations by Zhang et al. (Zhang et al., 2006).

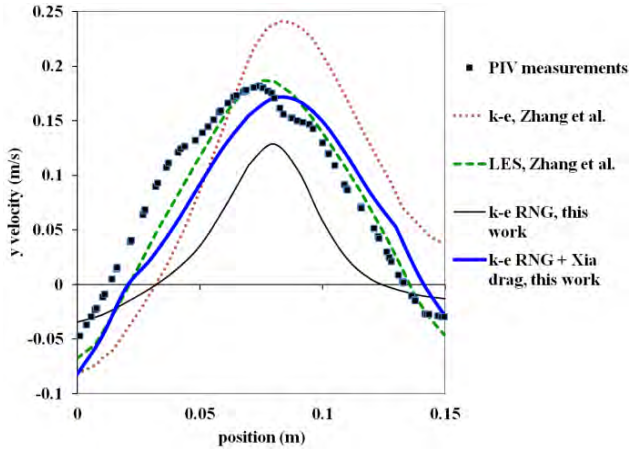


Figure 4: Velocity comparison along a centreline at $y=0.25$ m and present model with DPM+VOF approach for different drag and turbulence conditions.

The main validation process consisted on predicting flow velocities along a transversal centreline (x axis) at different y positions (height positions); and compare them to the experimental benchmark. The DPM+VOF model showed good overall agreement at a transversal line; $y=0.25$ m, when compared to PIV experiments in the benchmark, with a peak in positive y velocity (upwards) at the centre of the bubble column that decreases towards the exterior and switches to negative y velocity values (downwards) along the walls (Figure 4).

Furthermore, the standard spherical and non-spherical drag functions in FLUENT were compared to the VOF+DPM model with extra source terms added as UDF's. These are shown with the corresponding Figures from the benchmark for a variety of turbulence and flow conditions in Figure 5. The spherical drag law provided closer results to experiments when compared to the non-spherical approach with 0.5 and 0.75 shape factor coefficients. However, native spherical and non-spherical laws still under predict the spreading of the bubble column (Figure 5a-left and centre). The addition of modified drag, lift and virtual mass forces provided a better agreement with the benchmark; with minor differences in velocity magnitude, but capturing satisfactorily the bubble column spread and overall intensity (Figure 5b). This is due to the fact that the built-in spherical and non-spherical drag laws produce a more closely packed column; whereas, the modified drag law provides a more realistic spreading of bubbles. Consequently, the combination of DPM+VOF with modified source terms was used as base to simulate argon injection within the mould during continuous casting.

Once validated, the DPM technique was coupled to the “base” model developed previously by the authors. The model runs in transient mode until a stable flow is achieved (approximately 100-200 seconds after argon injection). This “stable period” is representative of the flow at a constant casting speed, fixed SEN immersion depth and constant cooling conditions (i.e. no casting speed ramping or SEN immersion depth changes).

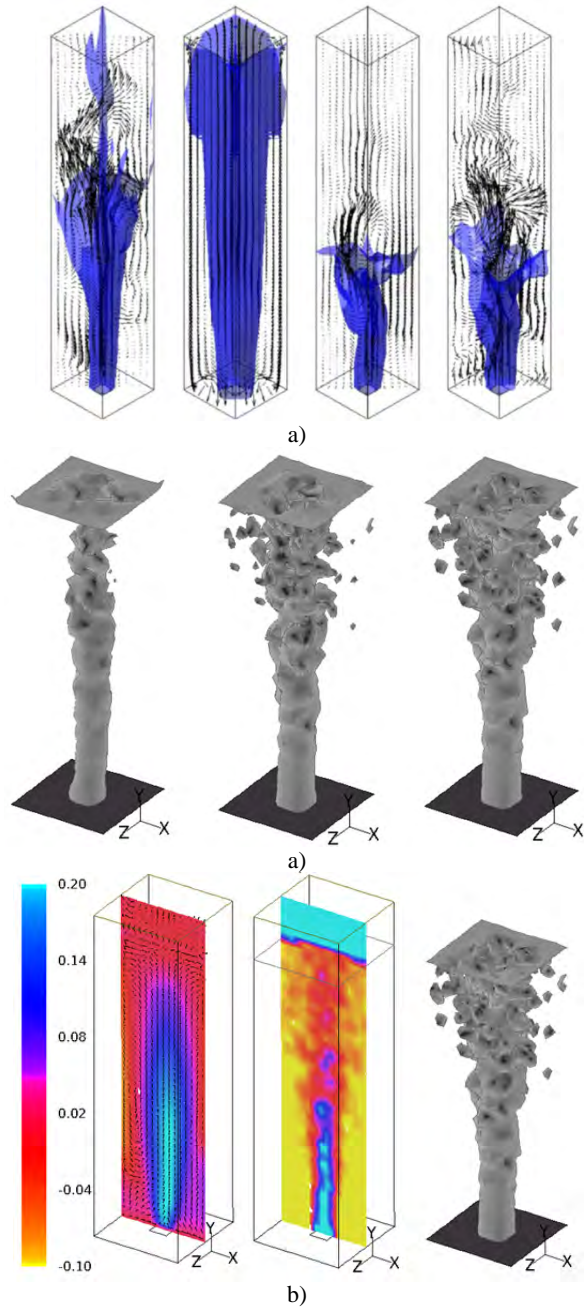


Figure 5: a) Comparison of bubble column spreading for different drag laws: a) Numerical simulations with several turbulence models after (Deen *et al.*, 2001; Zhang *et al.*, 2006) and b-c) Comparison of bubble column spreading for different drag laws: b) This work with standard functions (from left to right): Non-spherical with shape factor=0.5, Spherical and Additional source term; c) Column velocities and spreading for additional terms case.

Boundary conditions for argon injection (DPM model) are as follows:

- Inlet: single point at the nozzle top-centre
- SEN walls and solid surfaces: reflection
- Mould top and outlet of numerical domain: escape
- Metal-slag interface and slag bed: not preconditioned (free transit between boundaries)

PRELIMINARY RESULTS AND VALIDATION

2D Simulations show that injected argon bubbles travel rapidly to reach the SEN ports (~2 s), while the bubble distribution along the SEN bore is considerably irregular along most of the nozzle height. However, before leaving the nozzle, the bubbles accumulate around the upper port and are dragged into the mould by the metal as it leaves the nozzle.

After leaving the port, the bubbles are entrained by the discharging jet for a distance clearly related to the bubble size and argon-flow rate. A variety of tests were carried out to compare FLUENT's built-in drag and numerical schemes (accuracy control, two-way turbulence coupling, tracking scheme selection, etc.). Some of these predictions are shown in Figure 6.

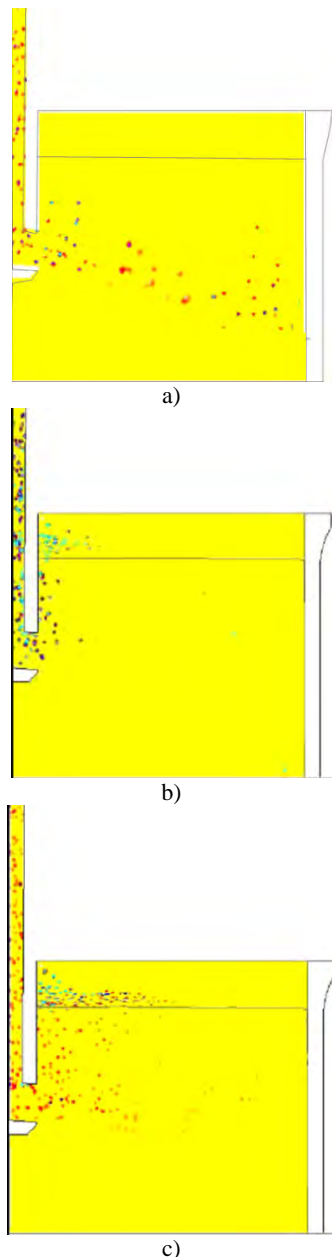


Figure 6: Fully developed bubble distribution for DPM+VOF model: a) DPM+VOF with Non-spherical-drag laws, bubble $\varnothing=2000\ \mu\text{m}$, b) DPM+VOF with Spherical-drag laws, bubble $\varnothing=2000\ \mu\text{m}$, and c) DPM+VOF with drag laws via UDFs', bubble $\varnothing=2000\ \mu\text{m}$.

Results demonstrate clearly that the only approach producing a realistic spreading of bubbles is the DPM+VOF+additional UDF's approach (Figure 6c). In contrast, the non-spherical drag laws cause total entrainment of bubbles along the discharging jet (Figure 6a), whereas the spherical laws cause departure of most bubbles close to the nozzle (Figure 6b). Simulations were performed to explore the influence of bubble size and different gas flow-rates in the calculations. For instance, Figure 7 shows the predicted velocity fields and bubble distribution for 4 and 5 lt/min at constant casting speed; which shows clear differences in bubble departure positions and flow behaviour. The 4 lt/min case produces a more even distribution of bubbles, which are entrained deeper into the melt by the discharging jet (Figure 7a). Thus, lower velocities close to the SEN are observed for the 4 lt/min case. In contrast, the 5 lt/min case leads to bubbles rising closer to the SEN due to coalescence and enhanced buoyancy and drag forces. Hence, bubbles leave "high velocity traces" when escaping the jet and reaching the surface. This creates higher departure velocities close to the SEN (e.g. dark red area adjacent to ports); and weakening of the discharging jet, which is also shorter and more distorted for the higher argon flow-rate (Figure 7b).

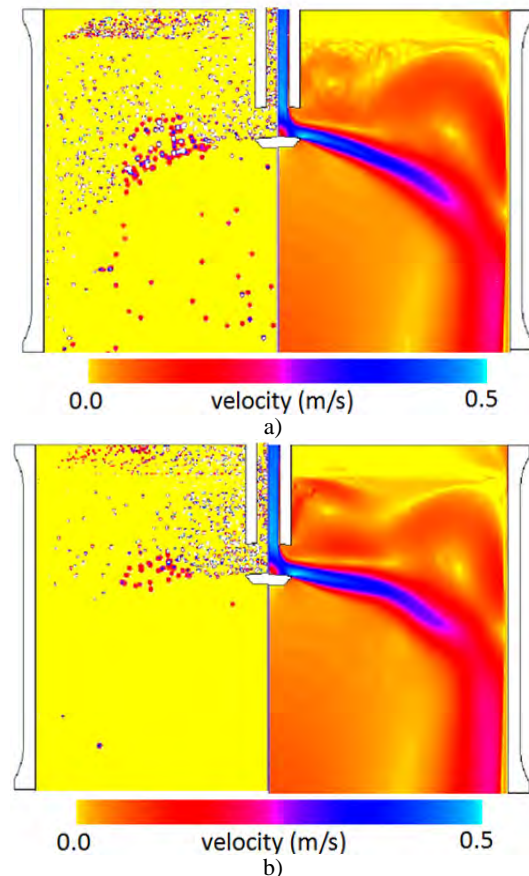


Figure 7: Simulated gas distributions and velocity fields for DPM+VOF model: a) Gas distribution for bubble $\varnothing=4\text{mm}$ and 4 lt/min and b) Gas distribution for bubble $\varnothing=4\text{mm}$ 5 lt/min.

This has deep implications when compared to the industrial praxis. Not incidentally, a transition from stable to unstable flow is detected when increasing the argon flow rate higher than 4.5 lt/min on industrial casters (which is the maximum gas flow rate employed

by operators for this particular case to avoid a “boiling effect” at the metal surface). Such *boiling effect* is known to be detrimental to mould level control due to unstable metal flows and produce more surface defects in the final product such as deep oscillation marks and cracks. This effect is a limiting factor since higher argon flow rates are desirable to improve flotation of inclusions but not at the expense of process stability. A key point on the simulations is the use of slag as secondary phase for the VOF model with properties that make it possible to distinguish between the liquid phase (slag pool), sintered layer and loose powder bed. The test runs with the improved model show that argon bubbles can reach the slag-metal interface, travel across it and exit the bed through the powdered layer with a corresponding change in bubble rising velocity through each of the slag layers due to viscosity changes (Figure 8).

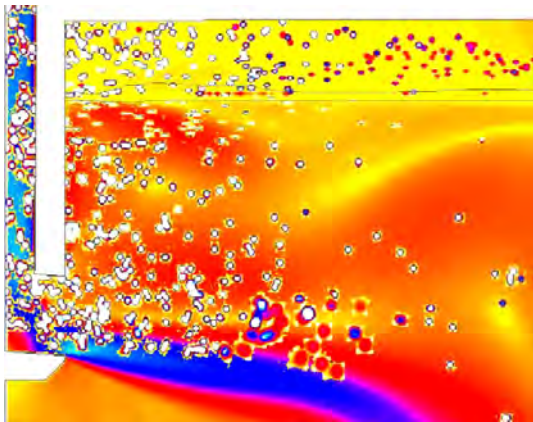


Figure 8: Argon bubble distribution and displacement through the slag-metal interface and through the slag with DPM+VOF embedded into existing CC model.

COMPARISONS WITH CASTING SIMULATOR (CCS-1)

Predictions of the average behaviour of the flow and bubbles once the flow stabilized were taken as basis for comparisons with a Continuous Casting Simulator (CCS-1) at Swerea MEFOS (Ramirez Lopez *et al.*, 2012). Designed and built between 2004-2007 during a RFCS project (Higson *et al.*, 2010), the model is equivalent to a continuous casting machine with tundish, stopper, Submerged Entry Nozzle (SEN) and mould. Hot metal is transported continuously from the tundish to the mould which is connected at the bottom to a heated tank/reservoir. A submerged pump sends the metal back from the tank to the tundish closing the flow loop (Figure 9). A low melting point alloy (58%Bi-42%Sn), is used as working media to simulate the steel flow, with properties described on Figure 10. The surface tension was defined as a function of temperature after (Aqra *et al.*, 2011; Man, 2000; Yuan *et al.*, 2002). Such alloy was chosen due to its close resemblance on fluid properties to steel and its non-toxicity. Electrical properties of the alloy are also close to liquid steel, which make it an ideal candidate for testing Electro-Magnetic Stirring (EMS) or Electro-magnetic Breaking (EMBr) devices as well as Electromagnetic sensors. The alloy’s melting point is approximately 135°C. Hence, temperature in the simulator is maintained within a few degrees to avoid solidification in the pump as well as

ensuring a smooth flow control by a stopper, which is controlled through a laser system. The simulator can use replicas in stainless steel of the stopper/SEN or the actual ceramic versions used on real casters. Stable operation for casting speeds between 0.6 to 1.4 m/min for a mould 900 x 200 mm size can be achieved. Higher casting speeds (c.a. 1.5-1.8 m/min) are possible by scaling the mould. Argon is supplied through the stopper tip for testing injection up to 8 lt/min.

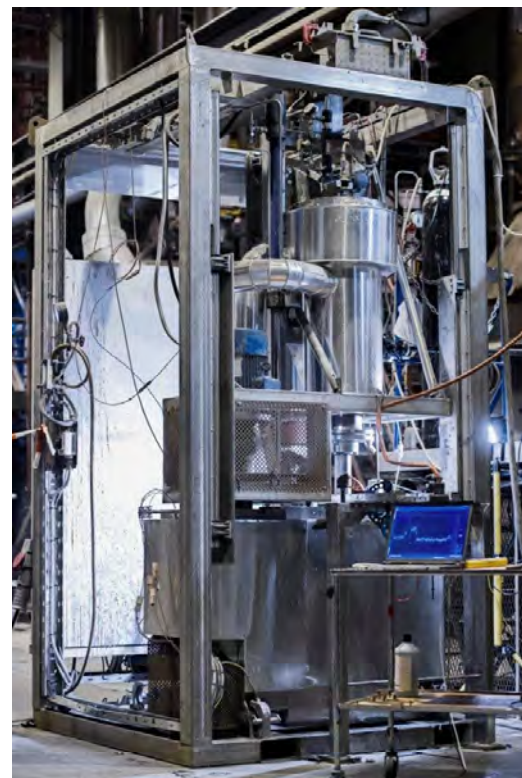
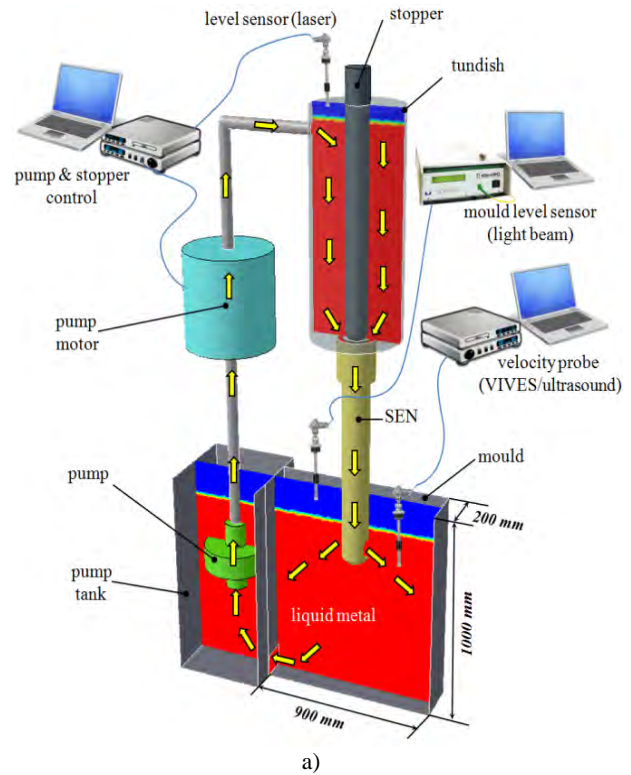


Figure 9: Continuous Casting Simulator CCS-1; a) Sensors and control schematics and b) Actual Continuous Casting Simulator at Swerea MEFOS

Bi-Sn alloy (MCP-137) properties compared to liquid steel				
	viscosity, μ (Pa-s $\times 10^{-3}$)	density, ρ (kg/m ³)	kinematic viscosity, ν (m ² /s $\times 10^{-6}$)	electrical conductivity, σ , (1/ Ω m $\times 10^6$)
Steel (1600 C°)	6.3	7000	0.9	0.7
MCP 137 (150 C°)	10.7	8580	1.25	1.0
MCP 137 (170 C°)	8.6	8580	1	

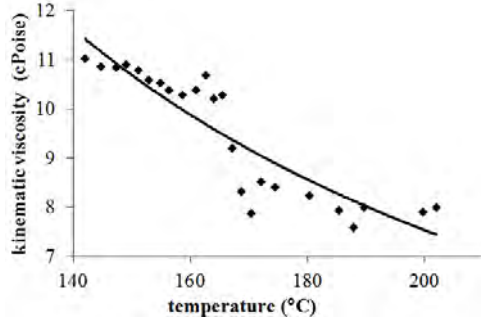


Figure 10: Properties of MCP 137 alloy vs steel and viscosity at operational temperatures

A variety of probes have been tested in order to find the most suitable tools to characterize the flow within the mould. Silicon oil was used to simulate the behaviour of liquid slag on top of the melt, while argon was supplied through the stopper-SEN (Figure 11).

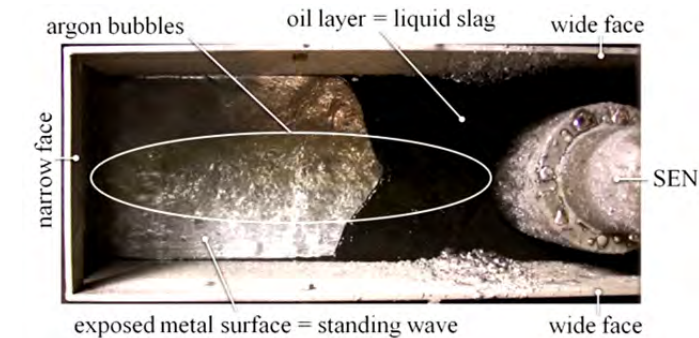


Figure 11: Top view of the metal level and oil simulating slag in CCS-1.



Figure 12: Video snapshots of the metal slag interface during argon injection tests at CCS-1 (taken every 10 seconds for a total time of 1 minute) for an argon mass flow rate=4 lt/min.

Observations of the metal level in CCS-1 at various flow-rates used typically during casting show that in all cases the bubbles have the following behaviour (Figure 11):

- Bubbles actually leave the metal bulk through the surface (opposite to results in Figure 6a).
- Bubbles are distributed along the whole metal surface (opposite to results in Figure 6b).
- Bubbles exit the metal surface along the whole mould width; with a higher amount bursting close to the SEN (in line with results on Figure 6c).

This demonstrates that the VOF+DPM approach with extra source terms is predicting realistically the behaviour of argon in the Casting Simulator and industrial practice. Furthermore, it is possible to deduce that the effect of higher argon flow-rates (e.g. from 4lt/min to 5lt/min) is an evident increase of instabilities in the mould due to bubble coalescence and augmented drag. In other words, the grouping of bubbles around the nozzle at higher argon loads would favour their collapse into larger bubbles, which offer a higher resistance to the discharging jet and reduce the number of smaller bubbles entrained deeper into the mould. This mechanism was observed by taking video sequences during tests in CCS-1 for the same argon flow rates: 4lt/min and 5 lt/min (Figures 12 and 13).

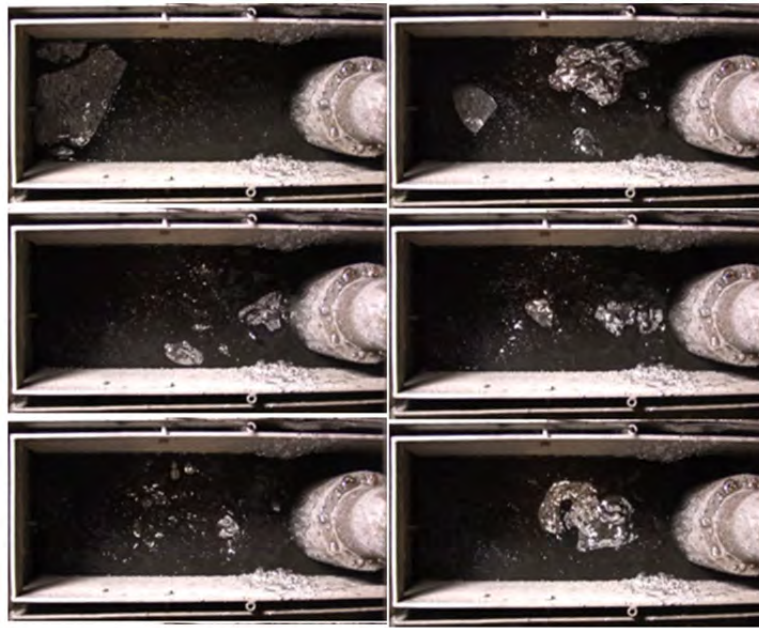


Figure 13: Video snapshots of the metal slag interface during argon injection tests at CCS-1 (taken every 10 seconds for a total time of 1 minute) for an argon mass flow rate=5 lt/min.

Differences in stability of the metal surface are easily noticeable by comparing the image-sequences. Lower argon flow rates produce a more stable flow pattern at the surface, with evidence of the well known “*double roll flow pattern*” (Ramirez-Lopez *et al.*, 2005) (e.g. upper roll pushing constantly the oil layer towards the nozzle).

In this case, argon bubbles depart uniformly along the mould width with smaller bubbles bursting closer to the narrow face; while slightly larger bubbles burst next to the SEN.

In contrast, a higher argon flow rate produces an unstable metal surface (e.g. random oil distribution) with some medium size bubbles bursting at random positions and large bubbles exploding close to the SEN. Comparison between 2D numerical models and CCS-1 are only qualitative. Therefore, 3D runs were performed to analyse the bubble distribution along the metal surface in a full numerical model of CCS-1 (Figures 14 and 15).

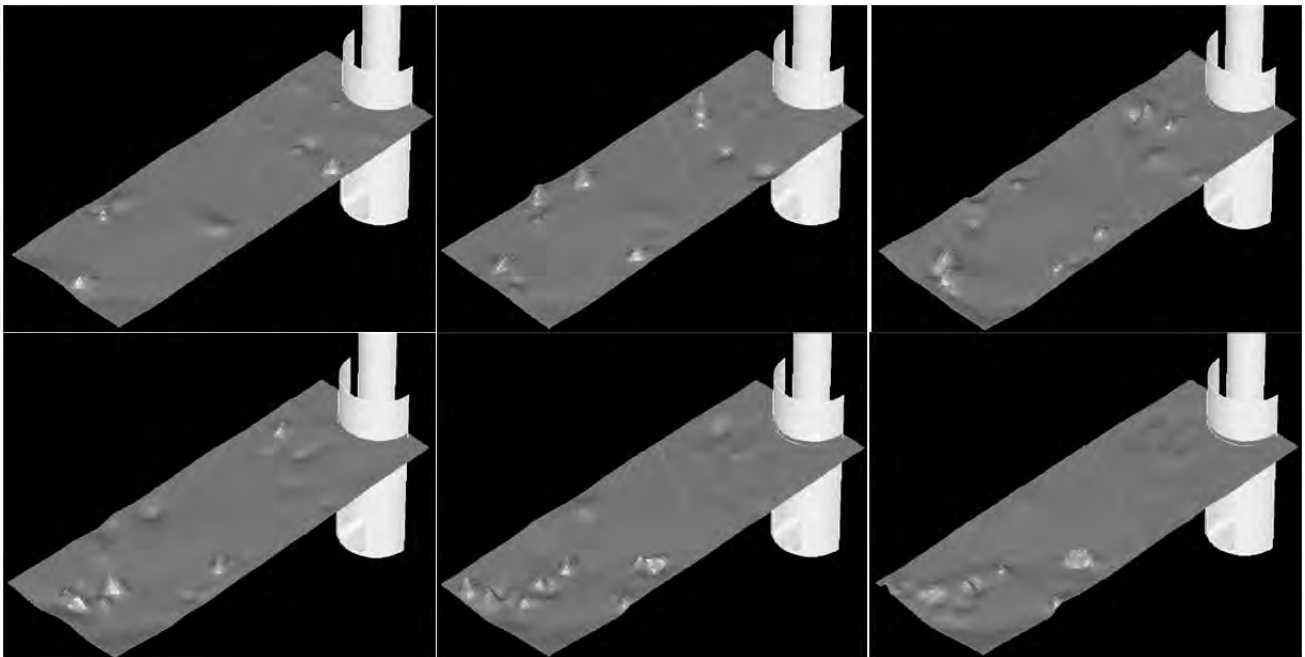


Figure 14: Snapshots every 0.5 s for a total of 3 s for 3D DPM+VOF model at 4lt/min and $v_c=1.2$ m/min.

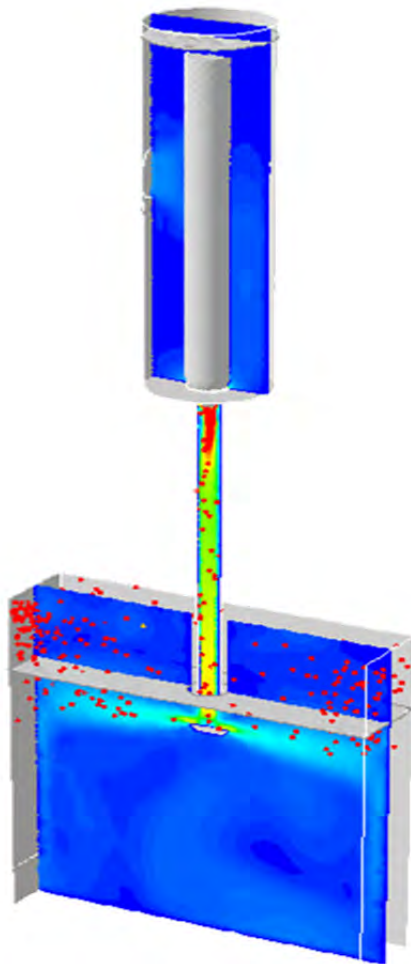


Figure 15: Numerical model of Continuous Casting simulator (CCS-1).

Tracking of the bubbles bursting at the metal surface was performed by counting the number of bubbles departing at different positions along the mould thickness and width (Figure 14). Statistics after 100 seconds show that approximately 60% of the bubbles depart close to a central plane parallel to the wide faces; while the rest burst randomly closer to the mould walls. It was also observed that more than 50% of the bubbles burst close to the SEN. These observations are in line with experiments in CCS-1 and previous plant experiences. This demonstrates that the 2D model is not far from the 3D case as long as slight corrections to the argon flow rate and bubble frequency are performed. This has significant implications for nozzle design and finding optimal argon flow rates for improved process windows. Analysis of these effects are ongoing tasks by means of parametric studies, further tests in CCS-1 and plant trials in a EU funded project (Ramirez Lopez *et al.*, 2013).

CONCLUSIONS

A numerical technique able to predict the multiphase (steel/slag) flow dynamics coupled with argon injection within the CC mould has been presented. The technique is based on the coupling of the DPM Lagrangian approach, which allows individual tracking of gas bubbles in a continuum phase; together with the Volume of Fluid method for calculation of free surfaces on multiphase flows.

The model has been developed with the aim of analysing industrial practices (e.g. argon injection) by comparing results with physical modelling in a Continuous Casting Simulator (CCS-1) and industrial observations. The following conclusions can be drawn from the application of these models:

- The coupling of the DPM technique to an existing CC model based on the multiphase VOF method has proven possible. This includes predictions of the displacement of bubbles across the slag-metal interface and through the slag bed covering the melt.
- The modified DPM+VOF model with additional source terms is capable of describing realistically the distribution of bubbles as seen in the casting simulator and industrial practice.
- Both the numerical and physical models presented are capable of matching phenomena observed in the industrial practice such as the “boiling effect” at excessive argon flow rates and standing waves which are detrimental to process stability as well as the typical double roll pattern seen in most casters.

The combination of predictions with the model developed and observations in CCS-1 allow a deeper understanding of the mechanisms responsible for achieving stable or unstable flows during casting. Findings provide enough evidence to consider the DPM+VOF technique as reliable for analysis of argon injection in the Continuous Casting process.

ACKNOWLEDGEMENTS

PRL would like to thank operators at SSAB for fruitful discussions, Mr. Christer Olofsson for support during CCS-1 trials and Mrs. Pilvi Oksman at Aalto University for proof-reading the manuscript. PJ would like to thank Professor Pär Jonsson at KTH, Stockholm for continuing support during his M.Sc. and Doctoral studies. The research leading to these results has received funding from the European Union's Research Programme of the Research Fund for Coal and Steel (RFCS) under grant agreement n° [RFSR-CT-2011-00005].

REFERENCES

- ANSYS-INC.: "ANSYS Fluent v.12 - User's Guide", ANSYS Inc., (2013),
- AQRA, F. and AYYAD, A.: "Surface tension of pure liquid bismuth and its temperature dependence: Theoretical calculations", *Materials Letters*, **65** (2011), 760-762.
- BRACKBILL, J.U., KOTHE, D.B. and ZEMACH, C.: "A continuum method for modeling surface tension", *Journal of Computational Physics*, **100** (1992), 335-54.
- CLOETE, S., OLSEN, J.E. and SKJETNE, P.: "CFD modeling of plume and free surface behavior resulting from a sub-sea gas release", *Applied Ocean Research*, **31** (2009), 220-225.
- CLOETE, S.W.P., EKSTEEN, J.J. and BRADSHAW, S.M.: "A mathematical modelling study of fluid flow and mixing in full-scale gas-stirred ladles", *Progress in Computational Fluid Dynamics*, **9** (2009), 345-356.
- CROSS, M., CROFT, T.N., DJAMBAZOV, G. and PERICLEOUS, K.: "Computational modelling of bubbles, droplets and particles in metals reduction and refining", *Applied mathematical modelling*, **30** (2006), 1445.

- DEEN, N.G., SOLBERG, T. and HJERTAGER, B.H.: "Large eddy simulation of the Gas-Liquid flow in a square cross-sectioned bubble column", *Chemical Engineering Science*, **56** (2001), 6341-6349.
- DÍAZ, M.E., IRANZO, A., CUADRA, D., BARBERO, R., MONTES, F.J. and GALÁN, M.A.: "Numerical simulation of the gas-liquid flow in a laboratory scale bubble column: Influence of bubble size distribution and non-drag forces", *Chemical Engineering Journal*, **139** (2008), 363-379.
- GHAJAR, A.J.: "Non-boiling heat transfer in gas-liquid flow in pipes: a tutorial", *Journal of the Brazilian Society of Mechanical Sciences and Engineering*, (2005),
- HIGSON, S.R., DRAKE, P., LEWUS, M., LAMP, T., KOCHNER, H., VALENTIN, P., BRUCH, C., CIRIZA, J., LARAUDOGOITIA, J., BJÖRKVALL, J. and BERGMAN, L.: "FLOWVIS: measurement, prediction and control of steel flows in the casting nozzle and mould", *EUR* **24205** (2010),
- IGUCHI, M., CHIHARA, T., TAKANASHI, N., OGAWA, Y., TOKUMITSU, N. and MORITA, Z.-I.: "X-ray fluoroscopic observation of bubble characteristics in a molten iron bath", *ISIJ International*, **35** (1995), 1354-1361.
- JOHANSEN, S.T., BOYSAN, F. and AYERS, W.H.: "Mathematical modelling of bubble driven flows in metallurgical processes", *Mathematical and Computer Modelling*, **10** (1988), 798.
- LIOW, J.L., RUDMAN, M. and LIOVIC, P.: "A volume of fluid (VOF) method for the simulation of metallurgical flows", *ISIJ international*, **41** (2001), 225-233.
- MAN, K.F.: "Surface tension measurements of liquid metals by the quasi-containerless pendant drop method", *International Journal of Thermophysics*, **21** (2000), 793-804.
- OLMOS, E., GENTRIC, C., VIAL, C.C. and WILD, G.: "Numerical simulation of multiphase flow in bubble column reactors. Influence of bubble coalescence and break-up", *Chemical engineering science*, **56** (2001), 6359.
- OLSEN, J.E. and CLOETE, S.W.P.: "COUPLED DPM AND VOF MODEL FOR ANALYSES OF GAS STIRRED LADLES AT HIGHER GAS RATES", *Seventh International Conference on CFD in the Minerals and Process Industries*, (2009), Melbourne, Australia
- PFEILER, C., WU, M. and LUDWIG, A.: "Influence of argon gas bubbles and non-metallic inclusions on the flow behavior in steel continuous casting", *Materials science & engineering. A, Structural materials*, **413-414** (2005), 115-120.
- RAMIREZ-LOPEZ, P.E., LEE, P.D., MILLS, K.C. and SANTILLANA, B.: "A new approach for modelling slag infiltration and solidification in a continuous casting mould", *ISIJ International*, **50** (2010), 1797-1804.
- RAMIREZ-LOPEZ, P.E., MORALES, R.D., SANCHEZ-PEREZ, R., DEMEDICES, L.G. and DAVILA, P.O.: "Structure of turbulent flow in a slab mold", *Metallurgical and materials transactions. B, Process metallurgy and materials processing science*, **36** (2005), 787-800.
- RAMIREZ LOPEZ, P.E.: "Modelling Shell and Oscillation Mark Formation during Continuous Casting via Explicit Incorporation of Slag Infiltration", **PhD Thesis**, Imperial College London (2010), 170.
- RAMIREZ LOPEZ, P.E., BJÖRKVALL, J., JONSSON, T., KARAGADDE, S., LEE, P.D., MILLS, K.C., VAN DER PLAS, D., VAN VLIET, E., SHAHBAZIAN, F., ANDERSSON, P., OPPELSTRUP, J., NILSSON, C. and WIKSTRÖM, P.: "Development of a toolbox for direct defect prediction and reduction through the characterisation of the meniscus-slag bed behaviour and initial shell solidification in CC", European-Commission, **RFSR-CT-2011-00005** (2013),
- RAMIREZ LOPEZ, P.E., BJÖRKVALL, J., SJÖSTRÖM, U., LEE, P.D., MILLS, K.C., JONSSON, B., JANIS, J., PETÄJÄRVI, M. and PIRINEN, J.: "EXPERIMENTAL VALIDATION AND INDUSTRIAL APPLICATION OF A NOVEL NUMERICAL MODEL FOR CONTINUOUS CASTING OF STEEL", *Ninth International Conference on CFD in the Minerals and Process Industries*, (2012), 1-6. Melbourne, Australia.
- RAMIREZ LOPEZ, P.E., JALALI NAZEEM, J., BJÖRKVALL, J., SJÖSTRÖM, U. and JÖNSSON, P.: "Recent Developments of a Numerical Model for Continuous Casting of Steel: Validation and Industrial Application", *3rd International Symposium on Cutting Edge of Computer Simulation of Solidification, Casting and Refining (CSSCR2013)*, (2013), Stockholm, SWEDEN and Helsinki, FINLAND.
- RAMIREZ LOPEZ, P.E., LEE, P.D. and MILLS, K.C.: "Explicit modelling of Slag Infiltration and Shell Formation during Mould Oscillation in Continuous Casting", *ISIJ International*, **50** (2010), 425-434.
- SPITZER, K., SCHWERDTFEGGER, K. and HOLZHAUSER, J.: "Laboratory study of heat transfer through thin layers of casting slag: Minimization of the slag/probe contact resistance", *Steel research*, **70** (1999), 430-436.
- THOMAS, B.G., DENNISOV, A. and BAI, H.: "Behavior of Argon Bubbles during Continuous Casting of Steel", *ISS 80th Steelmaking Conference*, (1997), Chicago, IL.
- TOMIYAMA, A.: "Drag, lift and virtual mass forces acting on a single bubble", *Proc. Third Int. Symp. on Two-Phase Flow Modelling and Experimentation*, (2004), Pisa, Italy.
- YUAN, Z.F., MUKAI, K., TAKAGI, K., OHTAKA, M., HUANG, W.L. and LIU, Q.S.: "Surface Tension and Its Temperature Coefficient of Molten Tin Determined with the Sessile Drop Method at Different Oxygen Partial Pressures", *Journal of Colloid and Interface Science*, **254** (2002), 338-345.
- ZHANG, D., DEEN, N.G. and KUIPERS, J.A.M.: "Numerical simulation of the dynamic flow behavior in a bubble column: A study of closures for turbulence and interface forces", *Chemical Engineering Science*, **61** (2006), 7593-7608.